Spell et al. 1990
ER ID # 21586

Volcanology and Geothermal Research, 43 (1990) 175–193
Elsevier Science Publishers B.V., Amsterdam

# $^{40}Ar/^{39}Ar$ dating of the Bandelier Tuff and San Diego Canyon ignimbrites, Jemez Mountains, New Mexico: temporal constraints on magmatic evolution

TERRY L. SPELL[a], T. MARK HARRISON[b] and JOHN A. WOLFF[c]

[a] *Dept. of Geological Sciences, State University of New York, Albany, NY 12222, U.S.A.*
[b] *Dept. of Earth and Space Sciences, University of California Los Angeles, Los Angeles, CA 90024, U.S.A.*
[c] *Dept. of Geology, University of Texas at Arlington Arlington, TX 76019, U.S.A.*

(Received August 30, 1989; revised and accepted January 18, 1990)

## Abstract

Spell, T.L., Harrison, T.M. and Wolff, J.A., 1990. $^{40}Ar^{39}Ar$ dating of the Bandelier Tuff and San Diego Canyon ignimbrites, Jemez Mountains, New Mexico: temporal constraints on magmatic evolution. *J. Volcanol. Geotherm. Res.*, 43: 175–193.

The Jemez Mountains volcanic field (JMVF), located in north-central New Mexico, has been a site of basaltic to rhyolitic volcanism since the mid-Miocene with major caldera forming eruptions occurring in the Pleistocene. Eruption of the upper Bandelier Tuff (UBT) is associated with collapse of the Valles Caldera, whereas eruption of the lower Bandelier Tuff (LBT) resulted in formation of the Toledo Caldera. These events were previously dated by K-Ar at 1.12 ± 0.03 Ma and 1.45 ± 0.06 Ma, respectively. Pre-Bandelier explosive eruptions produced the San Diego Canyon (SDC) ignimbrites. SDC ignimbrite "B" has been dated at 2.84 ± 0.07 Ma, whereas SDC ignimbrite "A", which underlies "B", has been dated at 3.64 ± 1.64 Ma. Both of these dates are based on single K-Ar analyses.

$^{40}Ar/^{39}Ar$ dating of single sanidine crystals from these units indicates revision of the previously reported dates. Isochron analysis of 26 crystals from the UBT gives a common trapped $^{40}Ar/^{36}Ar$ component of 304.5, indicating the presence of excess $^{40}Ar$ in this unit, and defines an age of 1.14 ± 0.02 Ma. Isochron analysis of 26 crystals from the LBT indicates an atmospheric trapped component and an age of 1.51 ± 0.03 Ma. An age of 1.78 ± 0.04 Ma, based on the weighted mean of 5 individual analyses, is indicated for SDC ignimbrite "B", whereas 3 analyses from SDC ignimbrite "A" give a weighted mean age of 1.78 ± 0.07 Ma. Evidence for xenocrystic contamination in the SDC ignimbrites comes from analyses of a correlative air-fall pumice unit in the Puye Formation alluvial fan giving ages of 1.75 ± 0.08 and 3.50 ± 0.09 Ma. The presence of xenocrysts in bulk separates used for the original K-Ar analyses could account for the significantly older ages reported.

Geochemical data indicate that SDC ignimbrites are early eruptions from the magma chamber which evolved to produce the LBT, as compositions of SDC ignimbrite "B" are virtually identical to least evolved LBT samples. Differentiation during the 270-ka interval between eruption of SDC ignimbrite "B" and the LBT produced an array of high-silica rhyolite compositions which were erupted to form the LBT. Mixed pumices associated with eruption of the LBT indicated an influx of more mafic magma into the system which produced shifts in some incompatible trace-element ratios. Lavas and tephras of the Cerro Toledo Rhyolite record the geochemical evolution of the Bandelier magma system during the 370-ka interval between eruption of the LBT and the UBT.

The combined geochronologic and geochemical data place the establishment and evolution of the

0377-0273/90/$03.50 © 1990 — Elsevier Science Publishers B.V.

7462

Bandelier silicic magma system within a precise temporal framework, beginning with eruption of the SDC ignimbrites at 1.78 Ma, and define a periodicity of 270–370 ka to ash-flow eruptions in the JMVF. The intervals are comparable to those in other multicyclic caldera complexes and are a measure of the timescales over which substantial fractionation of large silicic magma bodies occur.

## Introduction

Detailed and precise geochronological data are essential to understanding the petrologic and geochemical evolution of large crustal magma systems. The K-Ar method has been a favored technique for dating Tertiary and Quaternary volcanic rocks because of the low atmospheric contamination in unaltered potassium-bearing rocks and minerals (see Dalrymple and Lanphere, 1969). K-Ar dating, however, has several potential limitations, among which are the large sample size required (with the concomitant danger of xenocrystic contamination, particularly in rocks derived from explosive eruptions), and precision limited by uncertainties from sample heterogeneity, argon spike calibration, and potassium concentration measurements. Many of the limitations of K-Ar dating are circumvented by the $^{40}Ar/^{39}Ar$ method. Advantages of the $^{40}Ar/^{39}Ar$ method include the ability to detect trapped $^{40}Ar$, to test assumptions regarding closed-system behavior, and increased precision as ages are calculated from the measurement of an isotope ratio rather than separate determinations of K and Ar. Megrue (1973) first demonstrated that $^{40}Ar/^{39}Ar$ dating by laser fusion was possible. York et al. (1981) have applied this technique to mm-sized samples using a continuous laser and showed that results comparable to conventional step-heating analyses could be obtained. In conjunction with a high-sensitivity, low-background mass spectrometer, this method has the advantage of allowing high-precision dating of relatively small samples (e.g., phenocrysts from nearly aphyric glassy volcanic rocks). In addition, analysis of individual crystals can detect and circumvent the effects of xenocrystic contamination.

K-Ar analyses of rocks from the Jemez Mountains volcanic field were first performed by workers from the U.S. Geological Survey in the 1960's (Doell et al., 1968). Since that time, other K-Ar, fission track, and U-Th disequilibrium dates have been published by several investigators (e.g., Marvin and Dobson, 1979; Izett et al., 1981; Gardner and Goff, 1984; Self et al., 1988). However, no systematic geochronologic work using the $^{40}Ar/^{39}Ar$ method has been presented. This paper gives the results of $^{40}Ar/^{39}Ar$ dating (generally on single crystals) for the Otowi and Tshirege Members (lower and upper, respectively) of the Bandelier Tuff (nomenclature of Bailey et al., 1969) and the San Diego Canyon ignimbrites (nomenclature of Turbeville and Self, 1988) along with new geochemical data for these units. These data place the establishment and evolution of the Bandelier silicic magma system within a precise chronological setting, and provide an important constraint on dynamic models of magma evolution for this and other large continental silicic magma systems.

## Geologic setting and previous work

The Jemez Mountains volcanic field (JMVF), located in north-central New Mexico at the intersection of the Jemez lineament with the western margin of the Rio Grande rift, is a site of major Pleistocene caldera-forming eruptions (Fig. 1). Volcanism in the JMVF ranges from mid-Miocene (~16.5 Ma) to Recent and is related to ongoing extensional tectonics of the Rio Grande rift (Gardner and Goff, 1984: Aldrich et al., 1986). Rocks of the JMVF are formally assigned to the Keres Group (> 13 to 6 Ma), the Polvadera Group (> 13 to ~2 Ma), and the Tewa Group (< 2 Ma) (Bailey et al., 1969). A complete suite of lithologies ranging from basalt to high-silica rhyolite is present, although eruptive products since ~2 Ma have been almost entirely rhyolitic.

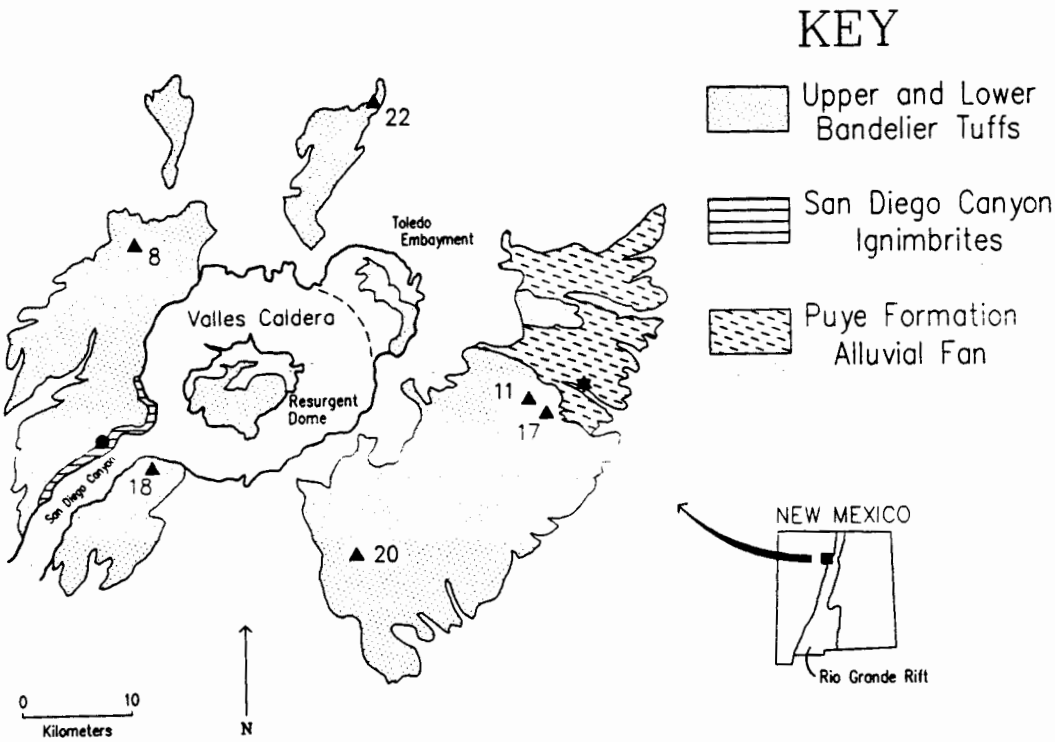


Fig. 1. Generalized geologic map of the Jemez Mountains volcanic field showing sample locations (partly after Smith et al., 1970). Sample locations: filled triangles = upper and lower Bandelier Tuffs, filled star = Puye Formation pumice fall, filled circle = San Diego Canyon ignimbrites.

The culminating phase of volcanism in the JMVF is represented by ash-flow eruptions which produced the San Diego Canyon (SDC) ignimbrites ( a lower unit "A", an upper unit "B"), and the Bandelier Tuff, consisting of the Otowi Member, or lower Bandelier Tuff (LBT), and the Tshirege Member, or upper Bandelier Tuff (UBT) (Smith and Bailey, 1968; Bailey et al., 1969; Self et al., 1986; Turbeville and Self, 1988). Eruption of the lower and upper Bandelier tuffs resulted in collapse of the Toledo and Valles calderas, respectively (Smith and Bailey, 1968; Bailey et al., 1969). The Toledo Caldera was originally thought to be represented by the Toledo embayment (Fig. 1). Subsequent work, however, has shown it to be roughly coincident with the Valles Caldera (Heiken et al., 1986). Recent drillhole data from the ongoing Continental Scientific Drilling Program in the Valles Caldera suggests that eruption of the SDC ignimbrites resulted in the formation of one or more calderas prior to the Toledo and Valles calderas (Nielson and Hulen, 1989). Post-Toledo/pre-Valles Caldera volcanism produced a sequence of rhyolite domes and tephras collectively named the Cerro Toledo Rhyolite (Bailey et al., 1969; Stix et al., 1988). Post-Valles Caldera volcanics consist of ring fracture rhyolite domes, composite domes, and pyroclastic rocks collectively designated the Valles Rhyolite Formation (Bailey et al., 1969; Self et al., 1988; Spell and Kyle, 1989).

Initial geochronology of volcanic rocks of the Jemez Mountains volcanic field was undertaken by Doell et al. (1968). They reported K-Ar dates of 1.12 ± 0.03 Ma for the upper Bandelier Tuff and 1.40 ± 0.04 Ma for the lower Bandelier Tuff based on analyses of sanidine separates (all ages are reported using decay constants and isotopic abundancs recommended by Steiger and Jäger, 1977) along with dates on lavas of the Valles

Rhyolite formation. Marvin and Dobson (1979) reported zircon fission-track dates on intracaldera rocks including one of the most recently erupted rhyolites, the Banco Bonito obsidian. Izett et al. (1981) presented the first K-Ar dates on Cerro Toledo Rhyolites and suggested the currently accepted ages for the upper and lower Bandelier Tuffs of 1.12 ± 0.03 Ma and 1.45 ± 0.06 Ma, respectively, based on weighted means of the data of Doell et al. (1968). Gardner and Goff (1984) published 20 new K-Ar dates, mainly on Keres Group rocks, and compiled most of the then available geochronologic data on the JMVF. Included in that paper was a date on a basanite (~16.5 Ma) from a sequence of alkali basalts interbedded with rift-related sediments of the Santa Fe Group which may represent the earliest eruptive activity in the Jemez Mountains area. Gardner et al. (1986) presented the most recent compilation of dates for the JMVF. Geochronologic data on the San Diego Canyon ignimbrites were first presented in an abstract by Kite et al. (1982). They reported K-Ar dates of 3.1–3.6 Ma for these units. These data were later published in a paper by Self et al. (1986) in which ages of 3.64 ± 1.64 Ma for SDC ignimbrite "A" and 2.84 ± 0.07 Ma for SDC ignimbrite "B" were reported (both dates on sanidine separates). The most recent geochronology on rocks of the JMVF is reported by Self et al. (1988) for the youngest eruptives, the El Cajete–Battleship Rock–Banco Bonito series. They suggested an age of 150 ± 30 ka for these rhyolites based on published fission-track ages and a U-Th disequilibrium date on the El Cajete pumice fall. A re-interpretation of the U-Th data, however, suggests a more probable age of ~350 ka (Self et al., in prep).

## Analytical methods

### *$^{40}Ar/^{39}Ar$ analyses*

Sanidine separates were obtained from whole pumice blocks by crushing, heavy liquid and magnetic separations, and hand picking. Individual crystals averaged 1–3 mg except for those from SDC ignimbrite "A" which were ~0.1 mg. Individual aggregates of crystals were kept to < 3 mm in height to avoid significant flux gradients across the packets. The Bern 4M muscovite (see Flisch, 1982) was used as a flux monitor. Large (~50 mg) monitors were placed at the center and at each end of the 4.5 cm quartz irradiation vial and small (~2 mg) monitors were placed between every other sample (at ~6-mm intervals). The correction for $^{40}Ar$ produced by the reaction $^{40}K(n,p)^{40}Ar$ was monitored using vacuum melted $K_2SO_4$. Samples and monitors were irradiated at the University of Michigan Ford reactor in a fast neutron flux of ~$5 \times 10^{12}$ n cm$^2$ s$^{-1}$ for 5 hours.

Samples and small flux monitors were analyzed using a VG 1200S mass spectrometer equipped with a GS-98 electron impact source and electron multiplier. Samples were fused with a 5-W Ar ion laser operated in the multi-line mode. The beam is steered by a series of mirrors, through a pyrex window, and focussed onto the crystals which are contained in a Cu dish. Sample viewing is accomplished by means of a binocular scope at an acute angle to the last leg of the laser path. The extraction system involves gas transfer by expansion and allows admission of ~50% of the gas to the mass spectrometer. Reactive gasses were removed with a 10–1 s$^{-1}$ SAES Ti-Zr getter operating at 0.85 A. Line blanks were typically $9.0 \times 10^{-17}$ mol $^{40}Ar$. A 0.1-mV correction at mass 36 was made to account for background associated with closing the inlet valve. Backgrounds were measured before each analysis and were relatively constant (e.g., 1.2–1.7 mV for mass 36). Sensitivity was typically $9.0 \times 10^{-18}$ mol/mV and an overall gain of ~100 is obtained with the multiplier operated at 1.75 kV. Peak height measurements are made over 6 cycles and extrapolated using a linear regression to give initial values. Individual analyses take ~25 minutes to complete.

The large flux monitors and $K_2SO_4$ were analyzed using a Nuclide 4.5-60-RSS mass spectrometer in Faraday cup mode. Correction fac-

tors used to account for interfering nuclear reactions were measured in the course of this study be $(^{40}Ar/^{39}Ar)_K = 0.0548$, $(^{36}Ar/^{37}Ar)_{Ca} = 0.00021$, and $(^{39}Ar/^{37}Ar)_{Ca} = 0.00075$.

J factors were determined from analyses of the large flux monitors at the ends of the irradiation vial. Analyses of the small (~2 mg) monitors showed large scatter and did not define the flux gradient established from the large monitors. Small monitors adjacent to large monitors gave J factors which differed by up to 10%. This suggests that the Bern 4M muscovite is inhomogeneous at the single crystal scale (2 mg monitors consisted of ~10–12 grains). Errors in J were assessed as ± 2% in contrast to the usual ± 1% as our normal practice of placing a monitor approximately every cm was not maintained due to the scatter shown by the small monitors.

We chose to take the age of the flux monitor, Bern 4M muscovite, as 17.9 Ma from the interlaboratory calibration of Dalrymple and Lanphere (1971) in order to avoid reporting differences due to differing calibrations (e.g., Flisch, 1982). Our results on the Bandelier tuffs and therefore directly comparable to those obtained by Doell et al. (1968).

*Geochemistry*

Whole pumice blocks were cleaned, powdered, and splits prepared for analysis. Following Wolff (1985), individual pumice clasts larger than 5 cm in diameter were used wherever possible. Samples taken from the plinian units of the lower and upper Bandelier tuffs (samples 11–16 and 8–34) consisted of clasts smaller than 5 cm, and several individual clasts from one level within the deposit were therefore combined to generate a single powder. A limited number of small (~100 mg) matrix glass separates were analyzed for trace elements by INAA. Detailed descriptions of sample preparation are given in Kuentz (1986) and Balsley (1988).

Major elements and Pb, Th, Rb, Sr, Y, Zr, Nb, Ga, Zn, and Ba were analyzed using an automated Rigaku 3062 XRF machine following the methods of Norrish and Hutton (1969) and Norrish and Chappel (1977). Other trace elements including the rare earth elements (REE) were analyzed by INAA following the procedures of Jacobs et al. (1977). Samples were irradiated at the University of Missouri Research Reactor for 40 hours at a flux of $2.2 \times 10^{13}$ n cm$^2$ s$^{-1}$ and counted after decay times of 7 and 35 days on two high-purity Ge detectors with resolutions of < 1.9 keV at 1332 keV and efficiencies of 18–25%. Data reduction was performed on a Nuclear Data 6620 system using a modified version of TEABAGS (Lindstrom and Korotev, 1982). Analytical precisions are generally better than ± 0.08 wt. % for major elements, ± 1.9 ppm for XRF trace elements, and ± 0.9 ppm for INAA trace elements. Further descriptions of analytical methods and estimates of precision are given in Kuentz (1986) and Balsley (1988).

## Results

*$^{40}Ar/^{39}Ar$ analyses*

Samples of the Bandelier Tuff were selected to cover the complete stratigraphy and range in high-silica rhyolite compositions within each of the two members (Table 1). Samples of low-silica rhyolite and dacite components of the upper Bandelier Tuff (discussed below) were not analyzed. Also included in Table 1 are samples of San Diego Canyon ignimbrites "A" and "B" along with two analyses of sanidine from a pumice fall unit near the top of the Puye Formation alluvial fan (Fig. 1) which has been correlated with SDC ignimbrite "B" on the basis of pumice morphology and trace-element chemistry (Turbeville and Self, 1988: Turbeville et al., 1989). All dates are on single crystals with the exception of those on SDC ignimbrite "A" and one of the correlative pumice fall analyses. Due to the small size of phenocrysts recovered from SDC ignimbrite "A" it was necessary to fuse 5–10 individual crystals in order to obtain a sufficient amount of gas for each analysis.

Ages based upon multiple single-crystal analyses were calculated by three methods. The

TABLE 1

$^{40}Ar/^{39}Ar$ data

| Sample | Wt. (mg) | $^{40}Ar/^{39}Ar$[2] | $^{37}Ar/^{39}Ar$[1] ($\times 10^{-2}$) | $^{36}Ar/^{39}Ar$[2] ($\times 10^{-3}$) | $^{39}Ar_K$ ($\times 10^{-15}$ mol) | $^{40}Ar^*$ (%) | $^{40}Ar^*/^{39}Ar_K$ | Age ± 1σ (Ma) |
|---|---|---|---|---|---|---|---|---|
| *UBT upper flow unit:* J = 0.0003740 | | | | | | | | |
| 20-55a | 1.76 | 2.149 | 1.495 | 1.55 | 4.61 | 74.9 | 1.624 | 1.10 ± 0.03 |
| 20-55c | 2.30 | 2.992 | 1.293 | 4.23 | 5.81 | 54.8 | 1.649 | 1.11 ± 0.03 |
| 20-55d | 1.49 | 2.941 | 1.612 | 4.22 | 3.67 | 53.9 | 1.603 | 1.08 ± 0.03 |
| 20-55f | 2.87 | 1.936 | 1.607 | 0.82 | 7.24 | 83.7 | 1.633 | 1.10 ± 0.02 |
| 20-55g | 1.60 | 2.250 | 0.973 | 1.95 | 3.87 | 70.3 | 1.608 | 1.08 ± 0.03 |
| 20-55h | 2.13 | 2.522 | 1.760 | 2.63 | 4.60 | 65.5 | 1.669 | 1.13 ± 0.04 |
| 20-55i | 1.34 | 2.032 | 1.383 | 0.91 | 3.31 | 82.4 | 1.702 | 1.15 ± 0.04 |
| 20-55j | 1.56 | 2.271 | 1.420 | 1.65 | 3.83 | 74.6 | 1.715 | 1.16 ± 0.04 |
| *UBT middle flow unit:* J = 0.0003675 | | | | | | | | |
| 22-50b | 2.81 | 2.827 | 0.955 | 3.48 | 7.07 | 60.3 | 1.712 | 1.13 ± 0.03 |
| 22-50c | 2.76 | 3.237 | 0.907 | 4.99 | 1.90 | 50.7 | 1.664 | 1.10 ± 0.08 |
| 22-50d | 3.00 | 4.135 | 0.958 | 7.91 | 7.19 | 40.3 | 1.672 | 1.11 ± 0.04 |
| 22-50f | 2.96 | 3.270 | 0.911 | 4.72 | 5.18 | 54.0 | 1.778 | 1.18 ± 0.04 |
| 22-50g | 4.36 | 2.342 | 0.861 | 1.85 | 10.87 | 73.3 | 1.725 | 1.14 ± 0.02 |
| 22-50i | 2.85 | 3.338 | 0.976 | 5.16 | 6.92 | 51.0 | 1.713 | 1.14 ± 0.03 |
| 22-50j | 2.32 | 2.725 | 0.983 | 2.98 | 5.09 | 64.2 | 1.762 | 1.17 ± 0.03 |
| 22-50k | 2.06 | 4.028 | 1.050 | 7.26 | 3.39 | 43.4 | 1.762 | 1.17 ± 0.04 |
| *UBT plinian:* J = 0.000370 | | | | | | | | |
| 8.34a | 3.01 | 2.493 | 0.864 | 2.33 | 7.78 | 69.1 | 1.732 | 1.16 ± 0.03 |
| 8.34b | 2.90 | 2.014 | 0.916 | 0.76 | 7.13 | 85.3 | 1.729 | 1.15 ± 0.03 |
| 8-34c | 2.46 | 2.467 | 0.990 | 2.34 | 6.12 | 68.4 | 1.700 | 1.13 ± 0.03 |
| 8-34d | 1.60 | 1.961 | 1.027 | 0.64 | 4.84 | 86.4 | 1.713 | 1.14 ± 0.03 |
| 8-34e | 2.08 | 2.543 | 0.960 | 2.54 | 5.27 | 66.8 | 1.714 | 1.14 ± 0.03 |
| 8-34f | 1.54 | 2.101 | 1.113 | 1.07 | 2.74 | 80.5 | 1.723 | 1.15 ± 0.04 |
| 8-34g | 1.88 | 1.951 | 0.940 | 0.69 | 4.43 | 85.3 | 1.685 | 1.12 ± 0.04 |
| 8-34h | 1.75 | 1.986 | 1.010 | 0.89 | 3.57 | 82.3 | 1.660 | 1.11 ± 0.03 |
| 8-34i | 1.73 | 2.070 | 0.862 | 1.13 | 3.18 | 89.5 | 1.672 | 1.12 ± 0.03 |
| 8-34j | 1.12 | 2.000 | 0.955 | 0.95 | 2.58 | 81.2 | 1.657 | 1.11 ± 0.04 |
| *LBT upper flow unit:* J = 0.000373 | | | | | | | | |
| 18-42a | 1.21 | 2.556 | 1.985 | 1.26 | 2.17 | 82.0 | 2.131 | 1.43 ± 0.05 |
| 18-42b | 2.49 | 2.465 | 1.585 | 0.60 | 5.79 | 90.1 | 2.235 | 1.50 ± 0.04 |
| 18-42c | 1.27 | 2.443 | 1.921 | 0.47 | 2.85 | 91.0 | 2.251 | 1.51 ± 0.04 |
| 18-42d | 2.48 | 2.378 | 1.809 | 0.14 | 3.70 | 95.1 | 2.284 | 1.54 ± 0.03 |
| 18-42e | 1.55 | 2.632 | 1.889 | 1.13 | 3.30 | 84.3 | 2.247 | 1.51 ± 0.05 |
| 18-42f | 1.21 | 2.491 | 2.261 | 0.85 | 2.45 | 86.3 | 2.188 | 1.47 ± 0.04 |
| 18-42g | 1.53 | 2.773 | 1.676 | 1.38 | 3.17 | 82.1 | 2.272 | 1.53 ± 0.04 |
| 18-42h | 1.54 | 2.802 | 2.021 | 1.83 | 3.46 | 78.0 | 2.209 | 1.49 ± 0.04 |
| 18-42i | 2.38 | 2.712 | 1.481 | 1.20 | 5.50 | 84.3 | 2.304 | 1.55 ± 0.04 |
| *LBT middle flow unit:* J =0.0003725 | | | | | | | | |
| 17-31a | 1.93 | 4.575 | 2.054 | 7.47 | 4.18 | 50.5 | 2.322 | 1.56 ± 0.06 |
| 17-31c | 3.55 | 4.829 | 1.719 | 8.52 | 8.79 | 46.8 | 2.265 | 1.52 ± 0.04 |
| 17-31e | 4.90 | 6.315 | 1.804 | 13.46 | 6.09 | 36.2 | 2.295 | 1.54 ± 0.05 |

TABLE 1 (continued)

| Sample | Wt. (mg) | $^{40}Ar/^{39}Ar$[2] | $^{37}Ar/^{39}Ar$[1] ($\times 10^{-2}$) | $^{36}Ar/^{39}Ar$[2] ($\times 10^{-3}$ | $^{39}Ar_K$ ($\times 10^{-15}$ mol) | $^{40}Ar^*$ (%) | $^{40}Ar^*/^{39}Ar_K$ | Age $\pm 1\sigma$ (Ma) |
|---|---|---|---|---|---|---|---|---|
| 17-31f | 1.74 | 5.627 | 1.555 | 11.11 | 4.03 | 40.6 | 2.297 | 1.54 ± 0.05 |
| 17-31g | 0.53 | 2.878 | 2.276 | 2.35 | 2.27 | 72.9 | 2.132 | 1.43 ± 0.07 |
| 17-31h | 2.56 | 4.872 | 1.898 | 9.00 | 5.27 | 44.3 | 2.166 | 1.45 ± 0.04 |
| 17-31j | 4.21 | 2.778 | 1.731 | 1.51 | 5.26 | 81.4 | 2.278 | 1.53 ± 0.04 |
| 17-31k | 2.45 | 4.542 | 1.726 | 7.80 | 5.54 | 48.0 | 2.191 | 1.47 ± 0.05 |
| 17-31m | 1.25 | 9.437 | 1.821 | 24.65 | 2.97 | 22.4 | 2.118 | 1.42 ± 0.07 |
| 17-31n | 1.09 | 5.086 | 2.250 | 9.29 | 2.55 | 44.8 | 2.296 | 1.54 ± 0.05 |
| *LBT plinian:* J = 0.000369 | | | | | | | | |
| 11-16a | 0.61 | 4.416 | 1.100 | 7.62 | 1.52 | 47.3 | 2.117 | 1.41 ± 0.06 |
| 11-16b | 1.45 | 3.085 | 1.155 | 2.76 | 1.89 | 70.3 | 2.212 | 1.47 ± 0.07 |
| 11-16c | 0.32 | 2.971 | 1.463 | 2.72 | 0.88 | 68.8 | 2.115 | 1.41 ± 0.10 |
| 11-16d | 1.18 | 3.008 | 0.887 | 2.21 | 2.08 | 75.5 | 2.303 | 1.53 ± 0.05 |
| 11-16f | 0.95 | 2.808 | 1.237 | 1.70 | 1.66 | 78.4 | 2.252 | 1.50 ± 0.06 |
| 11-16g | 0.52 | 2.872 | 1.623 | 2.14 | 1.23 | 73.9 | 2.189 | 1.46 ± 0.09 |
| 11-16i | 0.41 | 2.509 | 1.819 | 1.06 | 0.86 | 81.4 | 2.145 | 1.43 ± 0.08 |
| *SDC ignimbrite "B":* J = 0.0003715 | | | | | | | | |
| 861-11a | 0.99 | 3.057 | 4.018 | 1.44 | 1.81 | 82.9 | 2.580 | 1.73 ± 0.05 |
| 861-11b | 2.83 | 3.463 | 4.962 | 2.63 | 4.99 | 75.6 | 2.633 | 1.76 ± 0.05 |
| 861-11c | 3.02 | 3.615 | 3.255 | 2.74 | 1.27 | 74.7 | 2.754 | 1.84 ± 0.08 |
| 861-11e | 3.34 | 3.367 | 3.396 | 2.20 | 5.89 | 78.7 | 2.665 | 1.79 ± 0.04 |
| 861-11g | 3.84 | 2.985 | 4.896 | 0.82 | 5.48 | 89.6 | 2.693 | 1.80 ± 0.04 |
| *SDC ignimbrite "A":* J = 0.000372 | | | | | | | | |
| PB-Ab | ~0.40(5) | 7.151 | 6.167 | 15.46 | 0.79 | 34.8 | 2.533 | 1.70 ± 0.13 |
| PB-Ac | ~0.50(8) | 3.435 | 2.426 | 2.07 | 0.83 | 77.7 | 2.770 | 1.86 ± 0.13 |
| PB-Ad | ~0.70(10) | 3.317 | 3.190 | 2.08 | 1.30 | 77.8 | 2.650 | 1.78 ± 0.09 |
| *Puye Formation pumice fall:* J = 0.000324 | | | | | | | | |
| P-22a | 1.57 | 4.597 | 4.874 | 1.16 | 1.20 | 63.7 | 2.989 | 1.75 ± 0.08 |
| P-22b | 2.50(4) | 8.613 | 3.814 | 8.67 | 2.80 | 69.3 | 6.000 | 3.50 ± 0.09 |

[1] Corrected for $^{37}Ar$ decay.
[2] Blank corrected.
All analyses on single crystals except SDC "A" and one Puye Formation pumice fall analysis – number of crystals fused for these indicated in parenthesis after wt.

first is by the sample mean and standard deviation. Secondly, ages were calculated by the use of weighted means where weighting is by the inverse of the variance (Young, 1962). Finally, the spread in radiogenic yield within analyses from each unit allowed isochron ages to be determined using the York (1969) regression method.

When calculating an age from multiple analyses it is useful to have a method such as the weighted mean which accounts for the varying quality of individual analyses. The use of weighted means, however, should be applied only to data sets in which the variation is purely analytical (i.e., not produced by geological factors such as the presence of more than one age component or variable trapped compositions). To

assess whether our data conform to such a model we have plotted all analyses from the SDC ignimbrites, the LBT, and the UBT (Table 1) as a frequency distribution spectrum (Fig. 2). This diagram illustrates the narrow and Gaussian nature of the age distributions shown by the samples which indicates that samples from each unit comprise discrete populations and therefore the spread within the data is due only to analytical errors. One analysis of SDC ignimbrite "B" falls noticeably outside of the range of the others (Fig. 2). This analysis was excluded from ages calculated for this unit on the basis that it does not fit the isochron defined by the other analyses to within experimental error (i.e., MSWD = 4.5 if included). In calculating weighted mean ages, the mean of the data with analytical errors only was taken, then a 2% J factor error was added.

At the $2\sigma$ level, samples from different stratigraphic positions in the upper Bandelier Tuff give identical ages, as do those from the lower Bandelier Tuff, regardless of whether ages are calculated as means and standard deviations, weighted means and errors, or from isochrons. All analyses from each member have therefore been pooled to give an age based on the three samples from throughout each stratigraphic section.

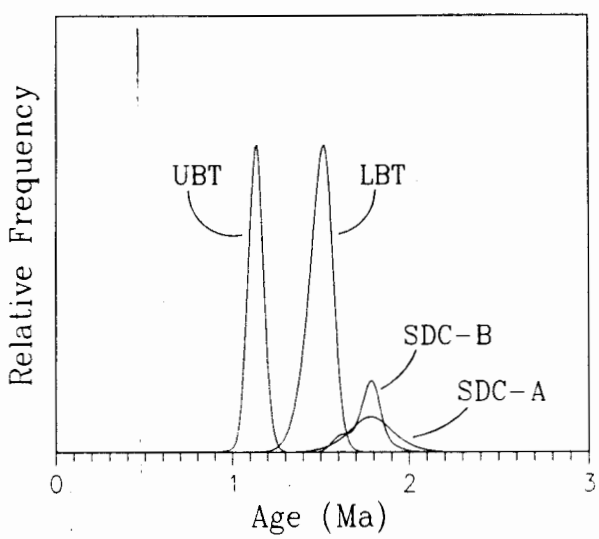


Fig. 2. Frequency distribution spectrum for $^{40}Ar/^{39}Ar$ ages determined in this study.

Ages calculated for San Diego Canyon ignimbrite "A" by the three methods are identical within analytical error (Table 2). The isochron age, however, is probably the least reliable as it is defined by only 3 points, two of which have virtually identical radiogenic yields (Table 1). Based on these three analyses the best estimate for the age of this unit is 1.78 ± 0.07 Ma from the weighted mean.

Five analyses from San Diego Canyon ignimbrite "B" define an isochron giving an age of 1.80 ± 0.05 Ma (MSWD = 1.26, $^{40}Ar/^{36}Ar$ = 284.7 ± 24.2), which is within error of the mean and weighted mean ages (Table 2). The variance in the $^{40}Ar/^{36}Ar$ intercept is large due to a relatively low spread in radiogenic yield of ~75–90% $^{40}Ar^*$. Therefore, the ages presented are calculated with an assumed trapped $^{40}Ar/^{36}Ar$ component of 295.5 (atmospheric), which is within error of the value indicated by the isochron. Based on these five analyses the best estimate for the age of this unit is 1.78 ± 0.04 Ma from the weighted mean.

Of two analyses of the airfall pumice unit on the Puye alluvial fan (sample P-22, Table 1) which Turbeville and Self (1988) correlate with SDC ignimbrite "B", one analyses gives an age of 1.75 ± 0.08 Ma, within the range of analysis for both SDC ignimbrites "A" and "B" (Table 1). The second analysis, in which 4 crystals were fused, yielded an age of 3.50 ± 0.09 Ma, indicating the presence of xenocrystic material in this unit.

When the analyses from the three stratigraphic positions within the lower Bandelier Tuff are normalized to a single J factor and plotted on an isochron, an age of 1.51 ± 0.03 Ma is indicated (Fig. 3). The data define a well correlated line (MSWD = 1.60) with a $^{40}Ar/^{36}Ar$ intercept of 294.7 ± 2.5, which is indistinguishable from atmospheric argon. All individual analyses of LBT samples reported in Table 1 are calculated using the trapped component defined by the isochron, however, use of the atmospheric value of 295.5 would have no effect on the ages calculated. As

TABLE 2

Compilation of $^{40}Ar/^{39}Ar$ ages calculated by sample mean and standard deviation, weighted mean, and isochron approaches

| Unit | Mean | Weighted mean | Isochron | $n$ |
|---|---|---|---|---|
| UBT | 1.13 ± 0.03 | 1.13 ± 0.02 | 1.14 ± 0.02 | 26 |
| LBT | 1.49 ± 0.05 | 1.51 ± 0.03 | 1.51 ± 0.03 | 26 |
| SDC-B | 1.78 ± 0.08 | 1.78 ± 0.04 | 1.80 ± 0.05 | 5 |
| SDC-A | 1.78 ± 0.08 | 1.78 ± 0.07 | 1.82 ± 0.05 | 3 |

Note: Errors reported at the 1$\sigma$ level.
UBT, upper Bandelier Tuff (Tshirege Member).
LBT, lower Bandelier Tuff (Otowi Member).
SDC-B, San Diego Canyon ignimbrite "B".
SDC-A, San Diego Canyon ignimbrite "A".

the isochron is well defined by a large number of data, it probably gives a realistic estimate of the uncertainty in this value. It is therefore appropriate to propagate this error into the estimate of the mean and weighted mean ages. As the mean age is not affected by uncertainty in individual ages its value remains as 1.49 ± 0.05 Ma, however, the age calculated by weighted mean takes a value of 1.51 ± 0.03 Ma (Table 2) (1.52 ± 0.03 Ma without inclusion of the trapped component error). We take the best estimate for the age of the LBT to be 1.51 ± 0.03 Ma based upon the isochron approach.

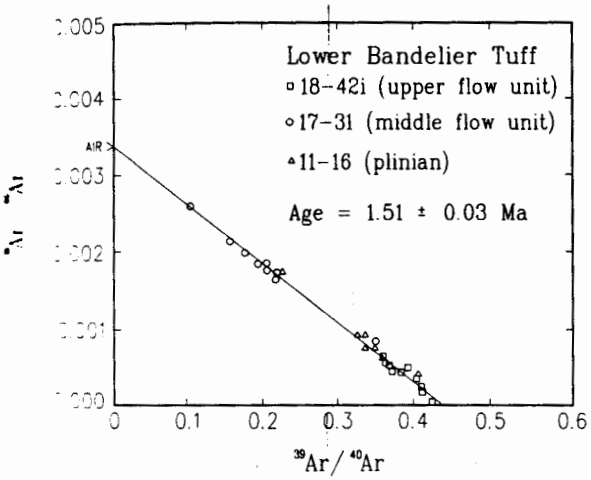


Fig. 3. Isochron plot for all samples from the lower Bandelier Tuff. $^{39}Ar/^{40}Ar$ ratios are normalized to sample 11-16 (J = 0.0003690).

As with the LBT, the analyses from the three stratigraphic positions within the upper Bandelier Tuff were normalized to one J factor and plotted on an isochron. These data define a well correlated line (MSWD = 1.35) which gives a $^{40}Ar/^{36}Ar$ intercept of 304.5 ± 4.5 and an age of 1.14 ± 0.02 Ma (Fig. 4). This isochron indicates a trapped component with a $^{40}Ar/^{36}Ar$ ratio slightly greater than atmospheric which is common to all crystals from the UBT. If this ratio is used to recalculate the individual analyses used in estimates of the mean and weighted mean the effect is to lower the individual ages by 0.5–4.0% depending upon radiogenic yield. The net effect

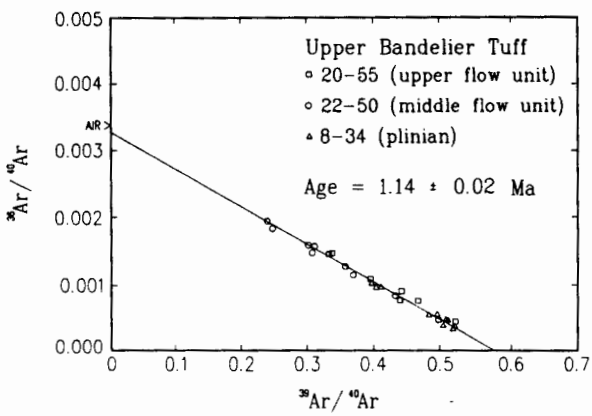


Fig. 4. Isochron plot for all samples from the upper Bandelier Tuff. $^{39}Ar/^{40}Ar$ ratios are normalized to sample 22–50 (J = 0.0003675).

TABLE 3

Major- and trace element geochemistry for dated and representative samples

| | UBT | | | LBT | | | PUYE | SDC-B | SDC-A |
|---|---|---|---|---|---|---|---|---|---|
| | 20-55 | 22-50 | 8-34 | 18-42i | 17-21 | 11-16 | 12-02a | 861-06 | PBA-01 |
| $SiO_2$ | 78.75 | 76.84 | 76.77 | 75.85 | 77.45 | 77.29 | 76.77 | 76.32 | 77.12 |
| $TiO_2$ | 0.07 | 0.06 | 0.06 | 0.08 | 0.08 | 0.04 | 0.09 | 0.12 | 0.13 |
| $AL_2O_3$ | 11.61 | 11.96 | 12.20 | 13.73 | 12.02 | 12.14 | 12.33 | 12.65 | 12.92 |
| $Fe_2O_3$* | 1.41 | 1.71 | 1.71 | 1.56 | 1.27 | 1.47 | 1.42 | 1.61 | 1.31 |
| MnO | 0.04 | 0.09 | 0.08 | 0.03 | 0.05 | 0.08 | 0.06 | 0.07 | 0.06 |
| MgO | 0.20 | 0.10 | 0.05 | 0.12 | 0.08 | 0.02 | 0.27 | 0.19 | 0.36 |
| CaO | 0.66 | 0.33 | 0.33 | 0.14 | 0.35 | 0.25 | 0.34 | 0.58 | 0.57 |
| $Na_2O$ | 2.70 | 4.34 | 3.54 | 2.65 | 3.91 | 4.30 | 3.30 | 3.25 | 3.14 |
| $K_2O$ | 4.54 | 4.57 | 5.25 | 5.83 | 4.79 | 4.39 | 5.50 | 5.20 | 4.37 |
| $P_2O_5$ | 0.023 | 0.008 | 0.013 | 0.010 | 0.013 | 0.006 | 0.013 | 0.010 | 0.050 |
| LOI | 4.05 | 3.35 | 2.98 | 3.90 | 2.69 | 4.25 | 4.62 | 2.70 | 1.89 |
| Rb* | 160.02 | 302.20 | 341.32 | 181.78 | 137.03 | 353.27 | 173.25 | – | – |
| Sr* | 19.59 | 12.96 | 20.75 | 5.46 | 5.74 | 3.23 | 6.8 | 5 | 8 |
| Y* | 89.31 | 120.41 | 142.56 | 65.86 | 43.63 | 117.13 | 45.83 | – | – |
| Zr* | 214.62 | 276.83 | 281.60 | 208.44 | 196.79 | 259.21 | 227.07 | – | – |
| Nb* | 75.45 | 151.52 | 152.92 | 90.65 | 62.45 | 186.68 | 65.80 | – | – |
| Ba* | 37.53 | 29.84 | 49.75 | 36.20 | 11.60 | 10.00 | 25.44 | 7 | 26 |
| Pb* | 36.36 | 51.37 | 51.46 | 15.32 | 15.98 | 47.06 | 25.79 | – | – |
| Zn* | – | – | 141 | 26 | 58 | 124 | 63 | 59 | 60 |
| Sc | 1.5 | 0.7 | 0.9 | 1.0 | 1.0 | n.d. | 2.0 | 2.4 | 2.1 |
| Cr | <0.4 | <0.2 | 2.6 | 1.9 | n.d. | n.d. | n.d. | 1.0 | 0.9 |
| As | 5.4 | 3.1 | 3.9 | 1.7 | n.d. | 4.4 | 1.7 | 1.9 | 1.4 |
| Sb | 0.14 | 0.49 | 0.50 | 0.26 | 0.20 | 0.53 | 0.42 | 0.19 | 0.19 |
| Cs | 4.20 | 9.60 | 14.30 | 5.90 | 3.02 | 10.48 | 8.30 | 3.59 | 3.91 |
| La | 94.1 | 52.2 | 52.9 | 49.9 | 47.7 | 38.7 | 50.0 | 52.4 | 40.0 |
| Ce | 157.3 | 115.2 | 111.3 | 94.8 | 96.0 | 94.5 | 100.4 | 102.5 | 78.1 |
| Nd | 69.8 | 42.3 | 44.4 | 34.7 | 34.6 | 41.1 | 32.4 | 35.3 | 26.3 |
| Sm | 15.4 | 11.2 | 11.0 | 9.0 | 6.7 | 11.0 | 7.2 | 7.4 | 6.3 |
| Eu | 0.428 | 0.056 | 0.082 | 0.121 | 0.078 | 0.015 | 0.156 | 0.127 | 0.210 |
| Tb | 2.28 | 2.71 | 2.71 | 1.69 | 1.11 | 2.65 | 1.12 | 1.21 | 1.11 |
| Yb | 7.40 | 11.40 | 11.23 | 6.00 | 4.10 | 10.70 | 4.16 | 4.35 | 4.26 |
| Lu | 1.08 | 1.67 | 1.66 | 0.93 | 0.67 | 1.61 | 0.63 | 0.66 | 0.63 |
| Hf | 8.40 | 14.20 | 13.70 | 8.20 | 7.00 | 13.50 | 7.80 | 7.60 | 6.99 |
| Ta | 5.3 | 10.7 | 10.7 | 7.0 | 4.9 | 14.4 | 5.0 | 4.5 | 4.7 |
| Th | 20.2 | 33.0 | 33.1 | 22.9 | 16.6 | 42.8 | 18.8 | 19.2 | 19.7 |
| U | 5.5 | 12.0 | 12.5 | 7.6 | 5.9 | 17.4 | 6.4 | 6.9 | 7.3 |

Note: Major elements normalized to 100% LOI free. Major elements in wt.%, trace elements in ppm, major elements and trace elements marked by* done by XRF, all other trace elements by INAA; Sr, Ba and Zn for SDC samples by ICP; $Fe_2O_3$*, total Fe as $Fe_2O_3$; LOI, loss on ignition; n.d., not detected; dash, not analyzed.

is to lower the mean age to 1.13 ± 0.03 Ma (Table 2) (down from 1.15 ± 0.03 Ma) and the weighted mean age to 1.13 ± 0.02 Ma (down from 1.15 ± 0.02 Ma). These values include propagation of the error in the trapped $^{40}Ar/^{36}Ar$ component, as indicated by the isochron. We take the best estimate for the age of the UBT to be 1.14 ± 0.02 Ma based upon the isochron approach.

*Geochemistry*

Major- and trace-element analyses of samples dated by the $^{40}Ar/^{39}Ar$ method along with selected other samples are presented in Table 3. A detailed discussion and interpretation of Bandelier Tuff geochemistry will be published elsewhere; aspects pertinent to the objectives of this study are summarized here.

The San Diego Canyon ignimbrites are characterized by phenocrysts of sanidine, quartz, pyroxene and magnetite. There are relatively few complete geochemical analyses of the SDC ignimbrites. Turbeville and Self (1988) present major element data for SDC ignimbrites "A" and "B" and INAA trace-element data for SDC ignimbrite "B" along with major and trace element data from the airfall deposit in the Puye alluvial fan correlative with SDC ignimbrite "B". Stix et al. (1988) also give analyses of two samples of the SDC ignimbrites. We present analyses of these units (Table 3) which are consistent with previously reported data. SDC ignimbrites "A" and "B" are virtually identical in major-element chemistry and are indistinguishable from the Puye pumice fall sample (Table 3). All are high-silica rhyolites ($SiO_2$ > 75 wt.% anhydrous) with relatively low abundances of CaO, MgO and MnO reflecting their evolved nature. Table 3 also shows the virtually identical trace-element abundances of SDC ignimbrite "B" and the Puye Formation pumice fall.

Phenocryst phases in the lower Bandelier Tuff include sanidine, quartz, fayalite, orthopyroxene, clinopyroxene, titanomagnetite, biotite, zircon and allanite. Chemically, the LBT consists of high-silica rhyolite of virtually constant major-element composition but up to four-fold variations in minor and trace elements (Table 3). Incompatible elements (e.g., Cs, Rb, Nb, Ta, Th, U, Yb, Lu) are highly correlated for both whole pumices and glass separates. A plot of Ta versus Th (Fig. 5) illustrates the wide compositional

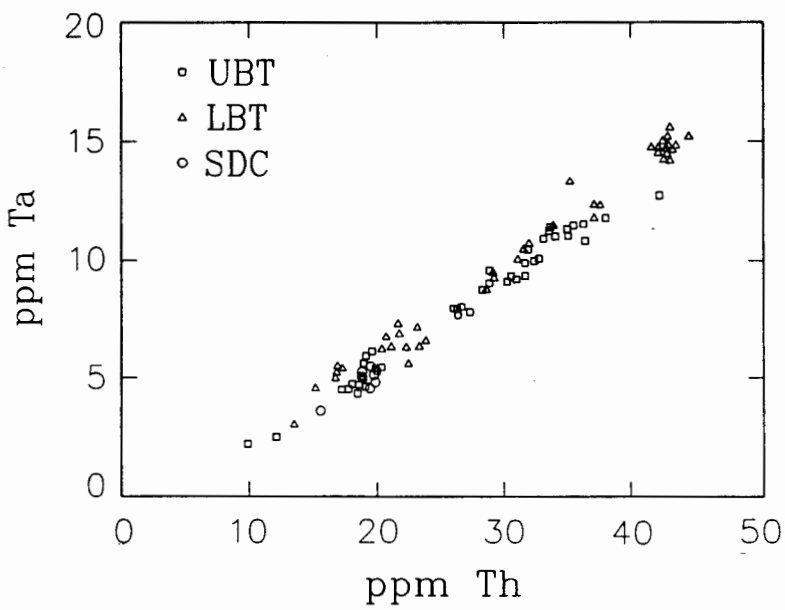


Fig. 5. Plot of Ta versus Th for samples the San Diego Canyon ignimbrites "A" and "B" (SDC), lower Bandelier Tuff (LBT), and upper Bandelier Tuff (UBT).

range seen in both LBT and UBT samples along with the restricted range of data from the SDC ignimbrites. Major- and trace-element compositions of the SDC ignimbrites are nearly identical to compositions of the least evolved lower Bandelier Tuff samples (Fig. 5, Table 3). Trace amounts of a more mafic composition in the LBT is found in mixed pumices with high-silica rhyolite (Kuentz, 1986). This more mafic component is geochemically distinct from the high-silica component in that it has higher ratios of REE to other trace elements.

Phenocryst phases present in the upper Bandelier Tuff include sanidine, quartz, titanomagnetite, ilmenite, fayalite, orthopyroxene, clinopyroxene, biotite, hornblende, chevkinite and apatite. The UBT is also composed dominantly of high-silica rhyolite of relatively constant major-element composition but widely varying trace-element abundances (Fig. 5, Table 3). Two other minor components are a grey dacitic (68–69 wt.% $SiO_2$) pumice found throughout the plinian and ignimbrite units and a low-silica rhyolite (72–73 wt.% $SiO_2$ pumice found only at a few locations (Balsley, 1988).

## Discussion

Single crystal dating of volcanic rocks by the $^{40}Ar/^{39}Ar$ method is a relatively recent development in geochronology. Accordingly, there is not yet a consensus on the treatment of data generated by this technique. Because large numbers of age measurements may now be used to calculate a date (20–30 measurements as opposed to 2–3 as has previously been common; e.g., Izett et al., 1981), a more sophisticated statistical treatment of data than has been necessary in the past may now be warranted.

The use of a sample mean and standard deviation as a statistical method for describing the central tendencies of data sets such as those presented here, is inferior to the use of a weighted mean for several reasons. The sample mean does not account for the varying quality of individual analyses and may therefore be affected by low-precision analyses near the limits of the range of data. A weighted mean allc higher-precision data to have correspondingly greater influence on an estimate of the mean than low-precision data and therefore de-emphasizes poor analyses. When dealing with repeated measurements of a quantity (i.e., the age of a rock) it may be argued that the larger the number of data that fall within specified limits, the more certain we may be of the mean value of those measurements. The weighted mean assigns a correspondingly lower standard deviation to a mean of measurements as their number increases, whereas a sample mean and standard deviation generally does not. In cases where the analytical precisions are much better than estimated errors in the J factor it is important to calculate the weighted mean using analytical errors, only, and apply J factor errors afterwards. This allows precise analyses proper influence in the mean determination, avoids quoting errors below that of the J factor, and is analogous to an age determination by the isochron method. Some workers have used the standard error of the mean (standard deviation/square root of numbe of measurements) as a measure of the precision of an age assessment derived from multiple single crystal analyses (Dalrymple and Duffield, 1988; Deino, 1989). The use of this statistic gives increasing precision with increasing number of analyses similar to the weighted mean used here, however, it suffers from the drawback discussed above as it is based on the sample mean and standard deviation.

We thus use weighted means of our data as the best estimates of the ages of units for which well defined isochrons are not available (SDC ignimbrites) and have suggested that this technique is appropriate where it is apparent that the data comprise discrete populations. Narrow, Gaussian profiles on a frequency distribution plot (Fig. 2) are suggestive that the data conform to such a restriction. Additional evidence that variations in the data are purely analytical may be obtained from isochron plots. MSWD values of 1.26, 1.35 and 1.60 for isochrons defined by ≥ 5

analyses indicate that the data fit the calculated line to within experimental error (e.g., McIntyre et al., 1966; McDougall and Harrison, 1988, and references therein). Also, the fact that the data fall on well defined isochrons indicates that all crystals from each unit share a common trapped component and a common radiogenic component and therefore comprise discrete populations. The presence of more than one trapped component (e.g., more than one population of crystals) results is a scatter of the data off of an isochron (Bogaard et al., 1987; Lo Bello et al., 1987).

The isochrons defined by analyses from the Bandelier tuffs are taken as the best estimates of the ages of these units as they are constrained by a large number of data points ($n$=26) with a large spread in radiogenic yield. The precisions of the isochron ages (and also of the weighted mean ages) are limited by poorly constrained J factors and would in fact easily be a factor of two higher with better control of flux monitoring.

The importance of isochron analysis is also illustrated for the case of the upper Bandelier Tuff in which a trapped $^{40}Ar/^{36}Ar$ component greater than atmospheric is indicated. Although marginally significant in this case (a decrease in weighted mean age of 1.4%), a higher value for the trapped component could result in a significant overestimation of the age and would go undetected without the use of isochrons. Also, well defined isochrons such as those presented for the UBT and LBT (Figs. 3 and 4) may allow assessment of an error for the value of the trapped $^{40}Ar/^{36}Ar$ component. This error may then be propogated into the calculation of weighted mean ages, thus giving more realistic estimates of the precision of such ages.

The data presented indicate minor revision of the ages of the upper and lower Bandelier Tuff and major revision of the ages of the San Diego Canyon ignimbrites. The currently accepted age for the upper Bandelier Tuff is 1.12 ± 0.03 Ma (Izett et al., 1981) based on the weighted mean of 3 K-Ar analyses from the data of Doell et al. (1968). Our results indicate a best estimate of the age of the UBT as 1.14 ± 0.02 Ma from isochron analysis. This estimate is a significant improvement in that it is based on a total of 26 analyses, includes samples from the range in stratigraphic position and high-silica rhyolite compositions shown by the UBT, and accounts for the non-atmospheric trapped $^{40}Ar/^{36}Ar$ component.

The currently accepted age for the lower Bandelier Tuff is 1.45 ± 0.06 Ma (Izett et al., 1981) based on the weighted mean of 3 K-Ar analyses from the data of Doell et al. (1968). Our results on the LBT indicate an age of 1.51 ± 0.03 Ma from isochron analysis. Once again, this estimate is based on a total of 26 analyses and includes samples from the range in stratigraphic position and chemical composition. In the case of the LBT, however, isochron analysis did not reveal the presence of a non-atmospheric trapped component.

Although our results on the Bandelier tuffs are within analytical error of the previously reported K-Ar dates, the data suggest that these units may be slightly older than previously thought. Our estimates of the ages of these units are 1.8% and 4.1% greater (UBT and LBT, respectively) than those proposed by Izett et al. (1981). Had the K-Ar ages for the UBT been calculated with the 304.5 trapped $^{40}Ar/^{36}Ar$ indicated by the isochron (Fig. 4), the discrepancy for this unit would be similar to that for the LBT. One explanation for this difference may be the difficulty of completely degassing high-temperature K-feldspars which are known to be quite retentive of radiogenic argon (e.g., Harrison and McDougall, 1982; McDowell, 1983). Incomplete degassing during a K-Ar analysis would lower the calculated age. McDowell (1983) suggests that ~2% of the $^{40}Ar^*$ may remain trapped in the melt even after heating at 1670 °C for 40 minutes. This may account for the ~3% apparent difference between the ages suggested by this work and previous K-Ar ages. Deino et al. (1989) have reported differences of up to 20% between K-Ar and $^{40}Ar/^{39}Ar$ ages for late Tertiary volcanic rocks in Nevada which they suggest may be attributed to this problem. It has been shown that high-temperature K-feldspars are

characterized by ideal flat age spectra yielding plateaus over virtually the entire temperature range of the step-heating experiment (Mc Dougall, 1981, 1985; Hess and Lippolt, 1986). This results from the fact that these samples have rarely been affected by a post-crystallization thermal event and therefore have a homogenous distribution of $^{40}Ar^*$. Thus, an advantage of the $^{40}Ar/^{39}Ar$ method when applied to volcanic samples is that a correct age should be obtained regardless of the degree of outgassing.

The previously reported age on San Diego Canyon ignimbrite "B" was 2.84 ± 0.07 based on a single K-Ar analysis (Self et al., 1986), whereas our data (weighted mean of 5 analyses) indicate an age of 1.78 ± 0.04 Ma. The previously reported age on San Diego Canyon ignimbrite "A" was 3.64 ± 1.64 Ma, also based on one K-Ar analysis. The large error on this age is due to the sample being only 4% radiogenic (Self et al., 1986). Data presented here (weighted mean of 3 analyses) indicates an age of 1.78 ± 0.07 Ma for SDC ignimbrite "A" which is identical to the age for SDC ignimbrite "B". The previously reported ages for the SDC ignimbrites suggests that contamination by xenocrystic material may have raised the K-Ar ages. One analysis from the Puye Formation pumice fall (sample P-22b, 3.50 ± 0.09 Ma) does show the effects of contamination by xenocrystic material, thus confirming its presence in these units. Sanidine analyzed from this unit was extracted from juvenile pumice blocks (as were all samples) and are not "lithic"material. The xenocrystic material in these rocks is thus cognate or accidental crystals which were incorporated into the magma prior to or during eruption. The age of 1.75 ± 0.08 Ma for the the other analysis from the Puye Formation pumice fall (Table 1) is identical to SDC ignimbrites "A" and "B", consistent with the interpretation of Turbeville and Self (1988) that this unit is correlative with SDC ignimbrite "B". In contrast to the SDC ignimbrites where the danger of xenocrystic contamination is evidently high (one analysis out of 10), we saw no evidence of this problem with either the UBT or the LBT (none out of a total of 52 analyses).

Smith (1979) suggested an age of ~1.5–2.0 Ma for the first appearance of "Bandelier magma" (SDC ignimbrites) based on enrichment rates for incompatible elements and stated that these eruptives probably represent "early leaks" from the Bandelier magma system. Self et al. (1986) also suggested that the SDC ignimbrites were early eruptives from the Bandelier magma system, and this is supported by close geochemical affinities of SDC and LBT pumices (see below). An age of 1.78 Ma for the onset of pre-Bandelier Tuff eruptive activity defines a consistent periodicity to ash-flow eruptions from the Bandelier magma system. The ages reported here yield a time interval between eruption of the SDC ignimbrites and the LBT of 270 ka, while the interval between eruption of the LBT and the UBT is 370 ka. These intervals compare with those for other multicyclic continental caldera systems. For example, seven ash-flow eruptions from the central caldera complex of the Cenozoic San Juan volcanic field, Colorado, occurred with a periodicity of 190–500 ka (averaging 360 ka) Lanphere, 1989). Existing K-Ar dating suggests that major ash-flow eruptions from the Miocene–Pliocene Timber Mountain–Oasis Valley caldera complex, Nevada, occurred with periodicities averaging ~480 ka (Broxton et al., 1989). Three caldera-forming eruptions in the Quaternary Yellowstone Plateau volcanic field occurred at intervals of 700 ka (Hildreth et al., 1984). In general, a review of the literature suggests that periodicities ranging from 100 to 700 ka, and averaging 300–500 ka, are common for caldera-forming eruptions from multicyclic silicic magma systems. These intervals provide a measure of the timescales over which substantial fractionation of large silicic magma bodies takes place.

Incompatible trace elements provide the most sensitive indicators of fractionation of these magmas. The geochemical behavior of the Bandelier silicic magma system from 1.78 to 1.14 Ma is illustrated in Figure 5. SDC ignimbrite units "A" and "B" are essentially composi-

tionally identical to each other and to least evolved LBT magmas (Th = 15–19 ppm). This suggests that the SDC ignimbrites represent magmas which were parental to the following LBT magmas. Fractionation to produce the most evolved LBT plinian compositions (Th = 43 ppm) occurred during the 270-ka interval separating SDC ignimbrite "B" from the LBT. The magma was variably fractionated with part of the volume remaining essentially unchanged during this time as indicated by the nearly identical least evolved LBT samples. These features are consistent with models of convective fractionation, where buoyant fractionated liquid, formed by crystallization against chamber walls, ascends as counterflow to the top of the system (McBirney, 1980; Sparks et al., 1984; Nilson et al., 1985; Thompson and Szekely, 1989; Tait et al., 1989). The main body of thermally convecting magma remote from the walls does not enjoy compositional change (or only on a much longer time scale than that required to initially form the fractionated capping layer).

The system experienced a minor influx of more mafic magma (found as dark streaks in mixed pumices) during the LBT eruption, with the effect of altering some trace element ratios in magmas sampled by post-LBT eruptions (Balsley et al., 1987). This influx appears not to have affected the behaviour of the most strongly incompatible elements such as Ta and Th (Fig. 5); relationships between these elements and Nb, U, Cs and Rb are similarly unaffected (Wolff, unpubl. data) and solely reflect fractionation processes. Stix et al. (1988) have presented geochemical data for the small-volume Cerro Toledo Rhyolite tephras and lavas which lie stratigraphically between the LBT and UBT. If these units represent the uppermost parts of the system, they may be regarded as monitors of progressive fractionation between the two Bandelier eruptions. For most of the lifetime of the series, the most evolved magma had 14–22 ppm Th (similar to the SDC, and dominant least evolved LBT and UBT high-silica rhyolite compositions), with limited enrichment of Th and other incompatible elements with time (Stix et al., 1988). During the stratigraphic interval between the uppermost Cerro Toledo tephra and the UBT, the upper parts of the magma chamber again became zoned to compositions having ca. 40 ppm Th, with some material remaining unfractionated. Whether or not this represents a genuine increase in the rate of fractionation is unclear given the precision of existing conventional K-Ar ages on Cerro Toledo units (and other problems with using the K-Ar method for dating young volcanic rocks, noted above). Nonetheless, the magma erupted to form the UBT exhibits the complete range of compositions from the magma present at the beginning of the differentiation cycle to the most evolved magma present just prior to eruption.

The combined geochemical and geochronologic data allow estimates of time-averaged concentration increase rates for incompatible trace elements in the uppermost part of the chamber during intervals between ash-flow eruptions. For these calculations the intervals between eruptions are taken as 270 ka (SDC ignimbrite "B" to LBT) and 370 ka (LBT to UBT). The average of three analyses from the correlative pumice fall in the Puye Formation is used as the starting composition from which the most fractionated liquids erupted during the LBT eruption (average of 13 analyses from the plinian phase) were produced. For the LBT to UBT interval an analysis of the lowermost tephra from the Cerro Toledo Rhyolite (Stix et al., 1988) was used as a starting composition whereas the average of 8 analyses of the plinian phase of the UBT eruption represents the most evolved liquids produced. Using these parameters the rates calculated for the SDC–LBT interval are 0.66 ppm/ka, 0.32 ppm/ka, 0.43 ppm/ka, 0.08 ppm/ka, and 0.02 ppm/ka for Rb, Y, Nb, Th, and Yb, respectively. Rates for the LBT–UBT interval are identical within uncertainties in age at 0.67 ppm/ka, 0.26 ppm/ka, 0.28 ppm/ka, 0.05 ppm/ka, and 0.02 ppm/ka for the same elements. These numbers are not quoted in order to imply a linear dependence of composition on elapsed time, but may be useful

for comparison with other systems having similar compositions and repose times.

The data presented here are consistent with the interpretation that the Bandelier magma system was established prior to eruption of SDC ignimbrites at 1.78 Ma and that from 1.78 to 1.14 Ma the chamber was a continuously evolving system which underwent differentiation during intervals between ash flow eruptions with only minor compositional modification by recharge during eruption of the LBT. In contrast, geochemical data along with Sr and Nd isotope data indicate that the Valles Rhyolite domes and tuffs (post-Valles Caldera eruptives) represent at least three successive new magma batches unrelated to the preceding upper Bandelier Tuff (Self et al., 1988; Spell and Kyle, 1989; Spell et al., 1989; Kyle, unpubl. data). This suggests a change from the maintenance and replenishment of a relatively large sub-caldera magma chamber to the emplacement and eruption of discrete smaller magma bodies which were vented from different spatial positions underneath the caldera.

Quantitative predictions from convective fractionation theory are difficult to evaluate, due to imprecise knowledge of relevant physical parameters such as magma viscosity and density, which for systems like the Bandelier are largely controlled by pre-eruptive magmatic water content. Making some simplifying assumptions, Wolff et al. (submitted) predict that the time required for the degree of zonation commonly seen in large continental silicic systems to develop is > 100 ka, which is consistent with the data presented in this paper. In the future, refinement of dynamic models and accurate estimates of magmatic water contents (e.g., Hervig and Dunbar, 1989), combined with precise geochronologic data such as reported here, will allow much more detailed understanding of the development and evolution of large silicic magma systems.

## Conclusions

(1) The best estimate for the age of the upper Bandelier Tuff is 1.14 ± 0.02 Ma based upon isochron analysis of 26 individual age determinations. This age is within analytical error of previous K-Ar determinations, but is more precise.

(2) The best estimate for the age of the lower Bandelier Tuff is 1.51 ± 0.03 Ma based on isochron analysis of 26 individual age determinations. This age is also within error of previous estimates, but is significantly more precise.

(3) The San Diego Canyon ignimbrites appear to have been erupted within a brief interval of time as no detectable difference in age between units "A" and "B" was found. The best estimates for the ages of these units are 1.78 ± 0.04 Ma (SDC ignimbrite "B") and 1.78 ± 0.07 Ma (SDC ignimbrite "A") based on weighted means of 5 and 3 analyses, respectively. An air-fall pumice unit in the Puye Formation alluvial fan is correlative with SDC ignimbrite "B" based on an age of 1.75 ± 0.08 Ma and trace element composition. Xenocrystic contamination in these rocks is suggested by an anomolously old age obtained on one sample of the air-fall pumice. This is the most probable cause of the discrepancy between the previous K-Ar dates (2.84 ± 0.07 Ma for "B" and 3.64 ± 1.64 Ma for "A") and the dates reported here.

(4) Major- and trace-element chemistry indicates that the SDC ignimbrites and the LBT and UBT were the products of a continuously evolving high-silica rhyolite magma chamber in which geochemical evolution was modified by eruption and recharge. Caldera-forming ash-flow eruptions from this system have occurred with a periodicity of 270–370 ka. Time-averaged enrichment rates for incompatible trace elements during the LBT–UBT interval were similar to those for the SDC–LBT interval.

## Acknowledgments

The geochemical data base from which part of this work is drawn was made possible by the assistance of P. Kyle at New Mexico Tech, and we also thank S.D. Balsley, J.N. Gardner, D.C. Kuentz, S. Self, C.E. Skuba and B.N. Turbeville for discussions and their contributions to the Bandelier project. This work was funded under DOE grant DE-FG02-87ER 137222 to TMH and grant DE-FG05-87ER 13795 to J AW. An earlier version of this manuscript benefitted from comments by F. Goff. We thank an anonymous reviewer for constructive comments which greatly improved the paper.

## References

Aldrich, M.J., Chapin, C.E. and Laughlin, A.W., 1986. Stress history and tectonic development of the Rio Grande Rift, New Mexico. J. Geophys. Res., 91: 6199–6211.

Bailey, R.A., Smith, R.L. and Ross, C.S., 1969. Stratigraphic nomenclature of volcanic rocks in the Jemez Mountains, New Mexico. U.S. Geol. Surv. Bull., 1274-P: 1–19.

Balsley, S.D., 1988. The petrology and geochemistry of the Tshirege Member of the Bandelier Tuff, Jemez Mountains Volcanic Field, New Mexico, U.S.A. M.S. thesis, University of Texas, Arlington, TX, 188 pp. (unpubl.).

Balsley, S.D., Wolff, J.A., Kuentz, D.C., Kyle, P.R. and Gardner, J.N.., 1987. The interrelationship of the upper and lower Bandelier Tuffs: Evidence from incompatible trace elements. EOS (Trans. Am. Geophys. Union), 68: 1512.

Bogaard, P.v.d., Hall, C.M., Schmike, H.-U. and York, D., 1987. $^{40}Ar/^{39}Ar$ laser dating of single grains: Ages of Quaternary tephra from the East Eifel Volcanic Field, FRG. Geophys. Res. Lett., 14: 1211–1214.

Broxton, D.E., Warren, R.G., Byers, F.M. and Scott, R.B., 1989. Chemical and mineralogic trends within the Timber Mountain – Oasis Valley caldera complex, Nevada: Evidence for multiple cycles of chemical evolution in a long-lived silicic magma system. J. Geophys. Res., 94: 5961–5985.

Dalrymple, G.B. and Duffield, W.A., 1988. High precision $^{40}Ar/^{39}Ar$ dating of Oligocene rhyolites from the Mogollon-Datil volcanic field using a continuous laser system. Geophys. Res. Lett., 15: 463–466.

Dalrymple, G.B. and Lanphere, M.A., 1969. Potassium-Argon Dating. Freeman, San Francisco, CA, 258 pp.

Dalrymple, G.B. and Lamphere, M.A., 1971. $^{40}Ar/^{39}Ar$ technique of K-Ar dating: A comparison with the conventional technique. Earth Planet. Sci. Lett., 12: 300–308.

Deino, A.L., 1989. Single-crystal $^{40}Ar/^{39}Ar$ dating as an aide in correlation of ash flows: Examples from the Chinmey Springs/New Pass Tuffs and the Nine Hill/Bates Mountain Tuffs of California and Nevada. N.M. Bur. Mines Miner. Resour. Bull., 131: 70.

Deino, A.L., Hausback, B.P., Turrin, B.T. and McKee, E.H., 1989. New $^{40}Ar/^{39}Ar$ ages for the Spearhead and Civet Cat members of the Stonewall Flat Tuff, Nye Co., Nevada. EOS (Trans. Am. Geophys. Union), 70: 1409.

Doell, R.R., Dalrymple, G.B., Smith, R.L. and Bailey, R.A., 1968. Paleomagnetism, potassium-argon ages, and geology of rhyolites and associated rocks of the Valles Caldera, New Mexico. Geol. Soc. Am. Mem., 116: 211–248.

Flisch, M., 1982. Potassium-argon analysis. In: G.S. Odin (Editor), Numerical Dating in Stratigraphy. Wiley, Chichester, pp. 151–158.

Gardner, J.N. and Goff, F., 1984. Potassium-argon dates from the Jemez Volcanic Field: Implications for tectonic activity in the north-central Rio Grande rift. N.M. Geol. Soc., 35th Annu. Field Conf. Guideb., pp. 75–81.

Gardner, J.N., Goff, F., Garcia, S. and Hagan, R.C., 1986. Stratigraphic relations and lithologic variations in the Jemez Volcanic Field, New Mexico. J. Geophys. Res., 91: 1763–1778.

Harrison, T.M. and McDougall, I., 1982. The thermal significance of potassium feldspar K-Ar ages inferred from $^{40}Ar/^{39}Ar$ age spectrum results. Geochim. Cosmochim. Acta, 46: 1811–1820.

Heiken, G., Goff, F., Stix, J., Tamanyu, G., Shafiqullah, M., Garcia, S. and Hagan, R., 1986. Intracaldera volcanic activity, Toledo Caldera and Embayment, Jemez Mountains, New Mexico. J. Geophys. Res., 91: 1799–1815.

Hervig, R.L. and Dunbar, N.W., 1989. Direct determinations of volatile gradients in the Bandelier Tuff through analysis of melt inclusions. N.M. Bur. Mines Miner. Resour. Bull., 131: 129.

Hess, J.C. and Lippolt, H.J., 1986. $^{40}Ar/^{39}Ar$ ages of tonstein and tuff sanidines: New calibration points for the improvement of the Upper Carboniferous time scale. Chem. Geol. (Isot. Geosci. Sect.), 59: 143–154.

Hildreth, W., Christiansen, R.L. and O'Neil, J.R.,

1984. Catastrophic isotopic modification of rhyolitic magma at times of caldera subsidence, Yellowstone Plateau Volcanic Field. J. Geophys. Res., 89: 8339–8369.

Izett, G.A., Obradovich, J.D., Naeser, C.W. and Cebula, G.T., 1981. Potassium-argon and fission-track zircon ages of Cerro Toledo rhyolite tephra in the Jemez Mountains, New Mexico. U.S. Geol. Surv., Prof. Pap., 1199-D: 37–43.

Jacobs, J.W., Korotev, R.L., Blanchard, D.P. and Haskins, L.A., 1977. A well tested procedure for instrumental neutron activation analysis of silicate rocks and minerals. J. Radioanal. Chem., 40: 93–114.

Kite, W.M., Self, S., Goff, F. and Wright, J.V., 1982. Pliocene explosive silicic volcanism in the Jemez Mountains, New Mexico. EOS (Trans. Am. Geophys. Union), 63: 1131.

Kuentz, D.C., 1986. The Otowi Member of the Bandelier Tuff: A study of the petrology, petrography, and geochemistry of an explosive silicic eruption, Jemez Mountains, New Mexico. M.S. thesis, Univ. of Texas, Arlington, TX, 165 pp. (unpubl.).

Lanphere, M.A., 1988. High resolution $^{40}Ar/^{39}Ar$ chronology of Oligocene volcanic rocks, San Juan Mountains, Colorado. Geochim. Cosmochim. Acta, 52: 1425–1434.

Lindstrom, D.J. and Korotev, R.L., 1982. TEABAGS: Computer programs for instrumental neutron activation analysis. J. Radioanal. Chem., 70: 439–458.

Lo Bello, Ph., Feraud, G., Hall, C.M., York, D., Lavina, P. and Bernat, M., 1987. $^{40}Ar/^{39}Ar$ step heating and laser fusion dating of a Quarternary volcanic from Neschers, Massif Central, France: The defeat of xenocrysic contamination. Chem. Geol. (Isot. Geosci. Sect.), 66: 61–71.

Marvin, R.F. and Dobson, S.W., 1979. Radiometric ages: Compilation B. U.S. Geol. Surv., Isochron West, 26: 3–32.

McBirney, A.R., 1980. Mixing and unmixing of magmas. J. Volcanol. Geotherm. Res., 7: 357–371.

McDougall, I., 1981. $^{40}Ar/^{39}Ar$ age spectra from the KBS Tuff, Koobi Fora, Lake Turkana, northern Kenya. Nature, 294: 120–124.

McDougall, I., 1985. K-Ar and $^{40}Ar/^{39}Ar$ dating of the hominid-bearing Pliocene-Pleistocene sequence at Koobi Fora, Lake Turkana, northern Kenya. Geol. Soc. Am. Bull., 96: 159–175.

McDougall, I. and Harrison, T.M., 1988. Geochronology and Thermochronology by the $^{40}Ar/^{39}Ar$ method. Oxford University Press, Oxford, New York, 212 pp.

McDowell, F.W., 1983. K-Ar dating: Incomplete extraction of radiogenic argon from alkali feldspar. Chem. Geol. (Isot. Geosci Sect.), 1: 119–126.

McIntyre, G.A., Brooks, C., Compston, W. and Turek, A., 1966. The statistical assessment of Rb-Sr isochrons. J. Geophys. Res., 71: 5459–5468.

Megrue, G.H., 1973. Spatial distribution of $^{40}Ar/^{39}Ar$ ages in lunar breccia 14301. J. Geophys. Res., 78: 3216–3221.

Nielson, D.L. and Hulen, J.B., 1989. New evidence for a concealed pre-Bandelier-age caldera in the western Valles Caldera complex, New Mexico. N.M. Bur. Mines. Miner. Resour. Bull., 131: 202.

Nilson, R.H., McBirney, A.R. and Baker, B.H., 1985. Liquid fractionation, II. Fluid dynamics and quantitative implications for magmatic systems. J. Volcanol. Geotherm. Res., 24: 25–54.

Norrish, K. and Chappell, B.W., 1977. X-ray fluorescence spectrometry. In: J. Zussman (Editor), Physical Methods in Determinative Mineralogy, 2nd ed. Academic, San Diego, CA., pp. 201–272.

Norrish, K. and Hutton, J.T., 1969. An accurate X-ray spectrographic method for the analysis of a wide range of geological samples. Geochim. Cosmochim. Acta, 33: 431–453.

Self, S., Goff, F., Gardner, J.N., Wright, J.V. and Kite, W.M., 1986. Explosive rhyolitic volcanism in the Jemez Mountains: Vent locations, caldera development, and relation to regional structure. J. Geophys. Res., 91: 1779–1798.

Self, S., Kircher, D.E. and Wolff, J.A., 1988. The El Cajete Series, Valles Caldera, New Mexico. J. Geophys. Res., 93: 6113–6127.

Self, S., Wolff, J.A., Skuba, C.E., Morrissey, M.M. and Spell, T.L., in prep. Revissions to the stratigraphy and volcanology of the post-0.5 Ma units and the volcanic section of VC-1 core hole, Valles Caldera, New Mexico. J. Geophys. Res.,

Smith, R.L., 1979. Ash-flow magmatism. Geol. Soc. Am., Spec. Pap., 180: 5–27.

Smith, R.L. and Bailey, R.A., 1966. The Bandelier Tuff: A study of ash-flow eruption cycles from zoned magma chambers. Bull. Volcanol., 29: 83–103.

Smith, R.L. and Bailey, R.A., 1968. Resurgent cauldrons. Geol. Soc. Am. Mem., 116: 613–662.

Smith, R.L., Bailey, R.A. and Ross, C.S., 1970. Geologic map of the Jemez Mountains, New Mexico. U.S. Geol. Surv. Map, I-571.

Sparks, R.S.J., Huppert, H.E. and Turner, J.S., 1984. The fluid dynamics of evolving magma chambers. Philos. Trans. R. Soc. London, Ser. A, 310: 511–534.

Spell, T.L. and Kyle, P.R., 1989. Petrogenesis of Valle Grande Member rhyolites, Valles Caldera, New Mexico: Implications for evolution of the Jemez Mountains magmatic system. J. Geophys. Res., 94:

10,379–10,396.

Spell, T.L., Kyle, P.R. and Thirwell, M., 1989. Geochemistry and Sr isotopic compositions of post-Bandelier Tuff rhyolites, Valles Caldera, New Mexico: Evidence for multiple magma systems in the Jemez Mountains Volcanic Field. N.M. Bur. Mines Miner. Resour. Bull., 131: 251.

Steiger, R.H. and Jäger, E., 1977. Subcommission on geochronology: Convention on the use of decay constants in geo- and cosmochronology. Earth Planet. Sci. Lett., 36: 359–362.

Stix, J., Goff, F., Gorton, M.P., Heiken, G. and Garcia, S.R., 1988. Restoration of compositional zonation in the Bandelier silicic magma chamber between two caldera-forming eruptions: Geochemistry and origin of the Cerro Toledo Rhyolite. J. Geophys. Res., 93: 6129–6147.

Wörner, S.R., Wörner, G., van den Bogaard, P. and Schmincke, H.-U., 1989. Cumulate nodules as evidence for convective fractionation in a phonolite magma chamber. J. Volcanol. Geotherm. Res., 37: 21–37.

Thompson, M.E. and Szekely, J., 1989. Density stratification due to counterbouyant flow along a vertical crystallisation front. Int. J. Heat Mass Transfer, 32: 1021–1036.

Turbeville, B.N. and Self, S., 1988. San Diego Canyon ignimbrites: Pre-Bandelier Tuff explosive rhyolitic volcanism in the Jemez Mountains, New Mexico. J. Geophys. Res., 93: 6148–6156.

Turbeville, B.N., Waresback, D.B. and Self, S., 1989. Lava-dome growth and explosive volcanism in the Jemez Mountains, New Mexico: Evidence from the Plio-Pleistocene Puye alluvial fan. J. Volcanol. Geotherm. Res., 36: 267–291.

Wolff, J.A., 1985. The effect of explosive eruption processes on geochemical patterns within pyroclastic deposits. J. Volcanol. Geotherm. Res., 26: 189–201.

Wolff, J.A., Wörner, G. and Blake, S., 1990. Gradients in physical parameters in zoned felsic magma bodies: implications for evolution and eruptive withdrawal. J. Volcanol. Geotherm. Res., 43: 37–55.

York, D., 1969. Least squares fitting of a straight line with correlated errors. Earth Planet. Sci. Lett., 5: 320–324.

York, D., Hall, C.M., Yanase, Y., Hanes,J.A. and Kenyon, W.J., 1981. $^{40}Ar/^{39}Ar$ dating of terrestrial minerals with a continuous laser. Geophys. Res. Lett., 8: 1136–1138.

Young, H.D., 1962. Statistical Treatment of Experimental Data. McGraw Hill, New York, NY, 172 pp.